

# Nanowire superconducting single-photon detectors on GaAs for integrated quantum photonic applications

**Citation for published version (APA):**

Gaggero, A., Jahanmirinejad, S., Marsili, F., Mattioli, F., Leoni, R., Bitauld, D., Sahin, D., Hamhuis, G. J., Nötzel, R., Sanjines, R., & Fiore, A. (2010). Nanowire superconducting single-photon detectors on GaAs for integrated quantum photonic applications. *Applied Physics Letters*, 97(15), 151108-1/3. Article 151108. <https://doi.org/10.1063/1.3496457>

**DOI:**

[10.1063/1.3496457](https://doi.org/10.1063/1.3496457)

**Document status and date:**

Published: 01/01/2010

**Document Version:**

Publisher's PDF, also known as Version of Record (includes final page, issue and volume numbers)

**Please check the document version of this publication:**

- A submitted manuscript is the version of the article upon submission and before peer-review. There can be important differences between the submitted version and the official published version of record. People interested in the research are advised to contact the author for the final version of the publication, or visit the DOI to the publisher's website.
- The final author version and the galley proof are versions of the publication after peer review.
- The final published version features the final layout of the paper including the volume, issue and page numbers.

[Link to publication](#)

**General rights**

Copyright and moral rights for the publications made accessible in the public portal are retained by the authors and/or other copyright owners and it is a condition of accessing publications that users recognise and abide by the legal requirements associated with these rights.

- Users may download and print one copy of any publication from the public portal for the purpose of private study or research.
- You may not further distribute the material or use it for any profit-making activity or commercial gain
- You may freely distribute the URL identifying the publication in the public portal.

If the publication is distributed under the terms of Article 25fa of the Dutch Copyright Act, indicated by the "Taverne" license above, please follow below link for the End User Agreement:

[www.tue.nl/taverne](http://www.tue.nl/taverne)

**Take down policy**

If you believe that this document breaches copyright please contact us at:

[openaccess@tue.nl](mailto:openaccess@tue.nl)

providing details and we will investigate your claim.

# Nanowire superconducting single-photon detectors on GaAs for integrated quantum photonic applications

A. Gaggero,<sup>1,a)</sup> S. Jahanmiri Nejad,<sup>2</sup> F. Marsili,<sup>2,3,b)</sup> F. Mattioli,<sup>1</sup> R. Leoni,<sup>1</sup> D. Bitauld,<sup>2,c)</sup> D. Sahin,<sup>2</sup> G. J. Hamhuis,<sup>2</sup> R. Nötzel,<sup>2</sup> R. Sanjines,<sup>3</sup> and A. Fiore<sup>2</sup>

<sup>1</sup>*Istituto di Fotonica e Nanotecnologie, CNR, Via Cineto Romano 42, 00156 Roma, Italy*

<sup>2</sup>*COBRA Research Institute, Eindhoven University of Technology, P.O. Box 513, 5600 MB Eindhoven, The Netherlands*

<sup>3</sup>*Ecole Polytechnique Fédérale de Lausanne (EPFL), Station 3 CH-1015 Lausanne, Switzerland*

(Received 30 July 2010; accepted 11 September 2010; published online 12 October 2010)

We demonstrate efficient nanowire superconducting single photon detectors (SSPDs) based on NbN thin films grown on GaAs. NbN films ranging from 3 to 5 nm in thickness have been deposited by dc magnetron sputtering on GaAs substrates at 350 °C. These films show superconducting properties comparable to similar films grown on sapphire and MgO. In order to demonstrate the potential for monolithic integration, SSPDs were fabricated and measured on GaAs/AlAs Bragg mirrors, showing a clear cavity enhancement, with a peak quantum efficiency of 18.3% at  $\lambda=1300$  nm and  $T=4.2$  K. © 2010 American Institute of Physics. [doi:10.1063/1.3496457]

The manipulation and transmission of quantum information opens avenues in the fields of computing and communications. Single photons are ideally suited for the transmission of quantum information at long distances due to their low decoherence rate, and are the basis of the commercial application of quantum information processing, i.e., quantum key distribution (QKD). Going beyond the simple QKD requires some level of single-photon manipulation. For example, the combination of single-photon sources, simple linear-optics circuits, and detectors can be used to build photonic quantum gates<sup>1,2</sup> and quantum repeaters for ultralong-distance QKD systems.<sup>3</sup> These applications would greatly benefit from the integration of different quantum photonic components on the same chip, leading to increased functionality and improved stability. Passive quantum photonic integrated circuits have also been demonstrated to provide quantum gates with very high stability.<sup>4</sup> However, such integration poses tremendous challenges, due to the very different and complex technologies employed. We propose here an approach to single-photon detection which is compatible with large scale integration with sources, microcavities, waveguides and interferometers. It is based on superconducting nanowires grown on GaAs heterostructures. Superconducting single-photon detectors (SSPDs),<sup>5</sup> based on the photon-induced creation of resistive regions (hot spots) in nanowires biased close to their critical current, have shown detection efficiencies of up to 30% at  $\lambda=1.3$   $\mu\text{m}$ , dark counts in the range of few hertz<sup>5</sup> and are extremely fast (with count rates approaching the gigahertz range).<sup>6,7</sup> SSPDs have so far been fabricated only on sapphire,<sup>5</sup> MgO,<sup>8</sup> and Si<sup>9</sup> substrates, which are not suitable for the integration with single photon sources. The fabrication of SSPDs on GaAs would enable integration with all the circuitry required for photonic quantum information processing, since GaAs readily lends itself to the large-scale production of single-photon sources,<sup>10</sup> waveguides, in-

terferometers, and phase modulators. Additionally, the integration of NbN nanowires with GaAs-based waveguides and microcavities can be used to increase the absorption in the thin film, leading to quantum efficiencies (QE) potentially approaching 100%. However, the use of GaAs as a substrate poses significant challenges for the SSPD fabrication, which requires the sputtering of high-quality ultrathin (3–5 nm) NbN films and the definition of narrow 100 nm and extremely uniform wires. The main problems are: (a) the mismatch between the substrate and NbN film lattice parameters is higher ( $\sim 28\%$ ) than with the other substrates used so far, (b) the best quality of NbN films is usually obtained with deposition temperatures ( $>800$  °C) incompatible with GaAs processing, (c) the relatively high atomic density of GaAs (as compared with sapphire or MgO) makes high-resolution electron beam lithography (EBL) challenging because of the stronger proximity effect. In the following we show that high-quality NbN films and nanowire devices can be obtained on GaAs despite the lattice mismatch. Furthermore, we demonstrate an example of monolithic integration with GaAs/AlAs microcavities, leading to enhanced quantum efficiency.

The deposition technique used is the dc reactive magnetron sputtering (planar, circular, balanced configuration) of a Nb target in a plasma containing  $\text{N}_2$  and Ar. Most deposition parameters are similar to our previous report<sup>11</sup>: pressure of the  $\text{N}_2$  and Ar mixture ( $3.3 \times 10^{-3}$  mbar with a 33%  $\text{N}_2$  partial pressure), cathode current (250 mA), and cathode voltage (590–640 V).

High substrate temperatures  $T_S > 800$  °C are used on sapphire substrates,<sup>5,8</sup> to promote the surface diffusion of the sputtered particles, resulting in films with high crystalline quality. We previously developed a low-temperature deposition process ( $T_S=400$  °C, quenched growth) on MgO, which yielded high quality NbN thin films.<sup>8</sup> However, films deposited on GaAs at  $T_S=400$  °C did not reach the same quality as the films on MgO.<sup>11</sup> We found that the reason of this degradation was that, at 400 °C, As oxide ( $\text{AsO}$  and  $\text{As}_2\text{O}_3$ ) evaporated from the GaAs substrate during the baking (6–8 h) and the deposition procedure (30 min), which resulted in

<sup>a)</sup>Electronic mail: alessandro.gaggero@ifn.cnr.it.

<sup>b)</sup>Present address: Department of Electrical Engineering and Computer Science, MIT, Cambridge, Massachusetts 02139, USA.

<sup>c)</sup>Present address: Photonics Theory Group, Tyndall National Institute, Lee Maltins, Prospect Row, Cork, Ireland.

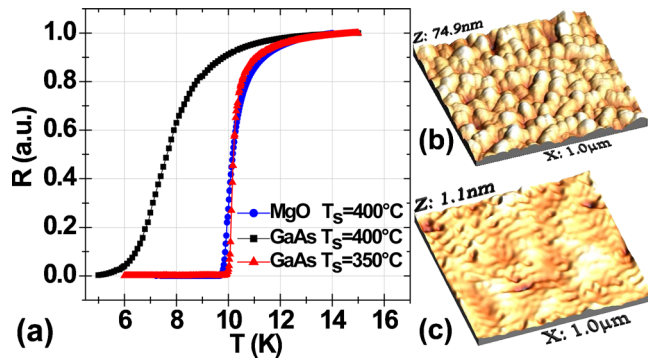


FIG. 1. (Color online) (a). Resistance vs temperature characteristics for different NbN films: 4.5 nm thick NbN film deposited on GaAs at  $T_S=400^\circ\text{C}$  (black squares); 4.0 nm thick NbN on MgO at  $T_S=400^\circ\text{C}$  (blue circles) and 4.5 nm thick NbN deposited on GaAs at  $T_S=350^\circ\text{C}$  (red triangles). All the thicknesses have been measured with AFM with a resolution of 0.5 nm as in [ref opex 08]. (b) AFM image of a 5 nm thick NbN film on GaAs deposited at  $T_S=400^\circ\text{C}$  and (c)  $T_S=350^\circ\text{C}$ .

poor morphology of the substrate surface and thus of deposited films. Indeed, evaporation of AsO starts at  $150^\circ\text{C}$ ,<sup>12</sup> and between  $300^\circ\text{C}$  and  $400^\circ\text{C}$  various chemical reactions take place, leading to the formation of a very stable  $\text{Ga}_2\text{O}_3$  oxide and evaporation of As and Ga from the substrate, which, due to the masking effect of the oxide, enhances surface roughness. Figure 1(a) shows the superconducting to normal transitions of  $\sim 4$  nm thick NbN films grown at  $T_S=400^\circ\text{C}$  on GaAs and MgO, all thicknesses are measured with atomic force microscopy (AFM) with an error of  $\pm 1$  nm. The NbN/MgO film has a high critical temperature  $T_c \approx 10.4$  K and transition width  $\Delta T_c \approx 1.0$  K, while on GaAs both a lower critical temperature ( $T_c \approx 6.8$  K) and a much wider transition ( $\Delta T_c \approx 2.4$  K) are observed. We investigated the surface morphology of NbN/GaAs films by AFM [see Figs. 1(b) and 1(c)]. A 5 nm thick NbN film grown at  $400^\circ\text{C}$  shows a very large granularity, with a grain size of about 100 nm, see Fig. 1(b). From the roughness analysis we obtain a root mean square roughness (rms roughness) of about  $\sim 10.9$  nm and a mean peak to peak distance of  $\sim 45$  nm while the peak to peak maximum value is  $\sim 75$  nm. We attribute this granularity to As-oxide desorption during baking, resulting in the formation of Ga or  $\text{Ga}_2\text{O}_3$  droplets,<sup>12</sup> as confirmed by a baking test performed on a GaAs substrate without NbN. The substrate granularity results in disordered superconducting films, where the localization of charge carriers by Coulomb interaction and the corresponding enhancement of quantum fluctuations of the phase of the superconductor order parameter induces the superconductor-insulator transition.<sup>13</sup> Lowering the baking and deposition temperature leads to a dramatic improvement of the surface quality and superconducting properties. Figure 1(c) shows the AFM images of a 4.5 nm NbN film deposited at  $350^\circ\text{C}$ , after a ( $200^\circ\text{C}$  for 12 h,  $350^\circ\text{C}$  for 30 min) baking sequence. The film shows a rms roughness of 0.126 nm and a mean peak to peak value 0.61 nm with the maximum peak to peak value of about 1.1 nm. This improvement in the microstructure has a direct effect on the superconducting transition. Indeed [see Fig. 1(a)], the transition width for 4.5 nm thick of the NbN film [Fig. 1(c)] is very narrow with  $\Delta T_c \approx 0.7$  K and the critical temperature is high ( $T_c \approx 10.3$  K). Besides, as expected, for a slightly thicker (5 nm) NbN film, the transition width is

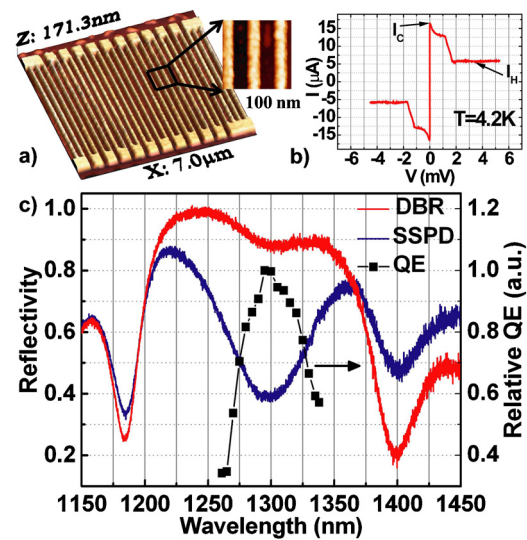


FIG. 2. (Color online) (a) AFM images a SSPD with  $w=100$  nm,  $t=5$  nm,  $f=40\%$ , and active area of  $5 \times 5$   $\mu\text{m}^2$  and detailed view of the SSPD NbN nanowire, coated with the HSQ mask; (b) Two-wires IV characteristic of the SSPD shown in (a) resulting in  $I_c=16.4$   $\mu\text{A}$  and  $I_H=5.9$   $\mu\text{A}$ . (c) Reflectivity (left axis) of the unprocessed DBR substrate (top continuous line), SSPD (lower continuous line), and spectral dependence of the QE (right axis) on a fabricated SSPD on DBR (squares).

narrower with  $\Delta T_c \approx 0.3$  K and the critical temperature is higher ( $T_c \approx 11.0$  K).

To further demonstrate the suitability of NbN/GaAs films for detector applications, we fabricated nanowire SSPD structures. On bare GaAs substrates, we measured QE of few percentages at 800 nm (not shown), due to the low detector optical absorptance ( $\alpha$ , calculated to be in the order of  $\approx 8\%$  in 4 nm thick nanowires with filling factor of 40%), due to the large index mismatch at the GaAs/air interface ( $n_{\text{GaAs}}=3.386$ ). In order to overcome this limitation, and to further show the compatibility of this NbN/GaAs technology with the growth and fabrication of conventional GaAs heterostructures, we have integrated a SSPD on top of a distributed Bragg reflector (DBR). The DBR was grown by molecular beam epitaxy on an undoped, (100)-oriented GaAs substrate, and consists of 14.5 periods of (113 nm AlAs/96.7 nm GaAs). It was capped by a 193.9 nm GaAs layer, acting as a  $\lambda/2$  spacer between the bottom Bragg mirror and the weak top mirror represented by the GaAs/air interface. The structure was designed to be resonant at 1309 nm under normal illumination at 4 K. Using a one-dimensional transfer matrix model of a meander (4 nm thick, filling factor 40%, polarization parallel to the wires) on the DBR [we modeled the meander as a uniform medium with average dielectric constant and assume a complex refractive index  $n=5.23+5.82i$  for NbN<sup>14</sup>] we calculated an absorptance of 83.2% at resonance. After DBR growth, NbN films with thicknesses in the 4–10 nm range were sputtered under the conditions described above, and nanowire SSPDs were defined using an EBL system equipped with a field emission gun (acceleration voltage 100 kV). The pattern was then transferred to the NbN film with a ( $\text{CHF}_3+\text{SF}_6+\text{Ar}$ ) reactive ion etching. Figure 2(a) shows an AFM image of a fabricated SSPD.

Figure 2(c) shows the reflectivity spectra (at 5 K, measured using a numerical aperture  $\text{NA}=0.5$ ) of the DBR before NbN deposition (red line, left axis), and of a SSPD fabricated from a 4.1 nm thick film (blue line, left axis, mea-



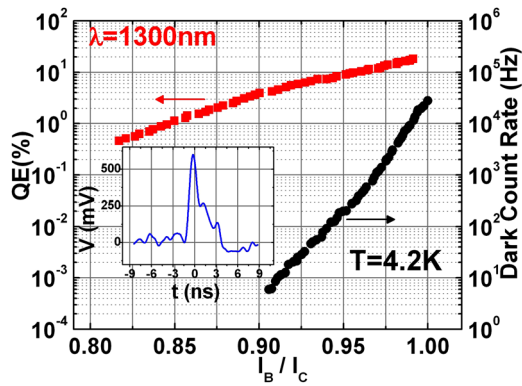


FIG. 3. (Color online) QE (squares, left axis) and dark count rate (circles, right axis) at 4.2 K as a function of the normalized bias current. The incident photon wavelength was 1300 nm. Inset: single-shot trace of SSPD output pulse after 56 dB amplification.

sured with light polarized parallel to the wires). The DBR reflectivity band extends from 1200 to 1370 nm, with a small dip around 1300 nm when no NbN film is present, which becomes much more pronounced after depositing and patterning the NbN nanowires. We attribute this difference to the absorption in the NbN wires. The current-voltage characteristic measured at liquid helium [Fig. 2(b)] shows a critical current  $I_c = 16.4 \mu\text{A}$ , corresponding to a critical current density  $J_c = 4.00 \text{ MA/cm}^2$ . During optical characterizations the polarization of the photons was controlled to maximize the number of detector counts, corresponding to an electric field parallel to the nanowires,<sup>14</sup> further details on measurement set-ups are reported in Refs. 8 and 15. The dependence of the number of detector counts per second on the average number of photons per pulse (not shown) was linear for the photon fluxes used in QE measurements, proof that true single photon detection was observed. The QE at a given bias current  $I_B$  (for the optimal polarization) was calculated as:  $\text{QE} = (N_c - \text{DCR}) / N_{\text{ph}}$ , where  $N_c$  is the number of detection events registered by the counter in one second,  $N_{\text{ph}}$  is the number of photons incident on the device area ( $\approx 5.5 \times 10^6 / \text{s}$ ) and DCR is the dark count rate at  $I_B$ , measured with the optical input blocked. The best measured device had a nanowire width,  $w = 100 \text{ nm}$ , filling factor  $f = 40\%$ , thickness  $t = 4.1 \text{ nm}$ , meander area  $S = 5 \times 5 \mu\text{m}^2$  and a sheet resistance at room temperature of  $R_{\square} \sim 570 \Omega/\text{sq}$ . Its QE (normalized to its peak value) is shown versus wavelength in Fig. 2(c) (symbols, right axis), as measured using a tunable laser in a cryogenic probe station,<sup>15</sup> with a device temperature  $T \approx 5\text{--}6 \text{ K}$  and a bias current  $I_B = 0.96I_c$ . A cavity resonance is observed, centered around 1300 nm, clearly corresponding to the reflectivity minimum. In this experiment the QE was low due to the unoptimized temperature and bias current.

The main panel in Fig. 3 shows the QE and DCR for the same device in a dip-stick<sup>8</sup> at 4.2 K under illumination at 1300 nm, while the output voltage pulse is shown in the inset. The usual<sup>8</sup> increase in both QE and DCR versus bias current is observed, with a maximum  $\text{QE} = 18.3\%$  at  $I_B = 0.99I_c$ , which is much higher than the calculated 8% absorptance of a 4 nm thick NbN film on a bare GaAs substrate, further confirming the effect of the cavity. From data showed in Fig. 3 we can estimate a NEP (noise equivalent power),<sup>16</sup> ranging from  $1.3 \times 10^{-17} \text{ W}/\sqrt{\text{Hz}}$  at  $0.91I_c$  (corresponding to a  $\text{QE} = 5.1\%$ ) to  $1.3 \times 10^{-16} \text{ W}/\sqrt{\text{Hz}}$  at  $0.99I_c$

(corresponding to a  $\text{QE} = 18.3\%$ ). The fact that the peak QE is lower than the theoretical absorptance of 83% and than previously reported QE values for microcavity SSPDs on sapphire<sup>17</sup> and silica<sup>18</sup> is ascribed to the limited internal quantum efficiency  $\eta$  ( $\eta$  is the probability that a photo-created hotspot produces a transition to the resistive state). Lower measurement temperatures and further fine tuning of the film thickness and deposition conditions should enable reaching a QE value equal to the absorptance.

In conclusion, we demonstrated SSPDs compatible with the well-developed III-V technology. These results will open the way to the realization of high-efficiency single-photon and photon-number-resolving<sup>19</sup> detectors integrated with waveguides and fully functional quantum photonic circuits.

We are grateful to H. Jotterand (EPFL) for technical support, to Dr. Thang B. Hoang (TU/e) for reflectivity measurements and to Professor G. Gol'tsman and Dr. A. Korneev for useful discussion. This work was supported by the European Commission through FP6 STREP "SINPHONIA" (Contract No. NMP4-CT-2005-16433), IP "QAP" (Contract No. 15848), and FP7 QUANTIP (Contract No. 244026).

<sup>1</sup>E. Knill, R. Laflamme, and G. J. Milburn, *Nature (London)* **409**, 46 (2001).

<sup>2</sup>M. A. Nielsen, *Phys. Rev. Lett.* **93**, 040503 (2004).

<sup>3</sup>N. Sangouard, C. Simon, J. Minář, H. Zbinden, H. de Riedmatten, and N. Gisin, *Phys. Rev. A* **76**, 050301 (2007).

<sup>4</sup>A. Politi, M. J. Cryan, J. G. Rarity, S. Yu, and J. L. O'Brien, *Science* **320**, 646 (2008).

<sup>5</sup>G. N. Gol'tsman, O. Okunev, G. Chulkova, A. Lipatov, A. Semenov, K. Smirnov, B. Voronov, A. Dzardanov, C. Williams, and R. Sobolewski, *Appl. Phys. Lett.* **79**, 705 (2001).

<sup>6</sup>M. Tarkhov, J. Claudon, J. Ph. Poizat, A. Korneev, A. Divochyi, O. Minaeva, V. Seleznev, N. Kurova, B. Voronov, A. V. Semenov, and G. Gol'tsman, *Appl. Phys. Lett.* **92**, 241112 (2008).

<sup>7</sup>F. Marsili, D. Bitauld, A. Gaggero, S. J. Nejad, R. Leoni, F. Mattioli, and A. Fiore, *New J. Phys.* **11**, 045022 (2009).

<sup>8</sup>F. Marsili, D. Bitauld, A. Fiore, A. Gaggero, F. Mattioli, R. Leoni, M. Benkhaoul, and F. Lévy, *Opt. Express* **16**, 3191 (2008).

<sup>9</sup>S. N. Dorenbos, E. M. Reiger, U. Perinetti, V. Zwiller, T. Zijlstra, and T. M. Klapwijk, *Appl. Phys. Lett.* **93**, 131101 (2008).

<sup>10</sup>A. J. Shields, *Nat. Photonics* **1**, 215 (2007).

<sup>11</sup>F. Marsili, A. Gaggero, L. H. Li, A. Surrente, R. Leoni, F. Lévy, and A. Fiore, *Supercond. Sci. Technol.* **22**, 095013 (2009).

<sup>12</sup>A. Guillén-Cervantes, Z. Rivera-Alvarez, M. López-López, E. López-Luna, and I. Hernández-Calderón, *Thin Solid Films* **373**, 159 (2000).

<sup>13</sup>Y. Dubi, Y. Meir, and Y. Avishai, *Nature (London)* **449**, 876 (2007).

<sup>14</sup>V. Anant, A. J. Kerman, E. A. Dauler, J. K. W. Yang, K. M. Rosfjord, and K. K. Berggren, *Opt. Express* **16**, 10750 (2008).

<sup>15</sup>D. Bitauld, F. Marsili, A. Gaggero, F. Mattioli, R. Leoni, S. J. Nejad, F. Lévy, and A. Fiore, *Nano Lett.* **10**, 2977 (2010).

<sup>16</sup>A. Korneev, V. Matvienko, O. Minaeva, I. Milostnaya, I. Rubtsova, G. Chulkova, K. Smirnov, V. Voronov, G. Gol'tsman, W. Slys, A. Pearlman, A. Verevkin, and R. Sobolewski, *IEEE Trans. Appl. Supercond.* **15**, 571 (2005).

<sup>17</sup>K. M. Rosfjord, J. K. W. Yang, E. A. Dauler, A. J. Kerman, V. Anant, B. M. Voronov, G. N. Gol'tsman, and K. K. Berggren, *Opt. Express* **14**, 527 (2006).

<sup>18</sup>M. G. Tanner, C. M. Natarajan, V. K. Pottapenjara, J. A. O'Connor, R. J. Warburton, R. H. Hadfield, B. Baek, S. Nam, S. N. Dorenbos, E. Bermúdez Ureña, T. Zijlstra, T. M. Klapwijk, and V. Zwiller, *Appl. Phys. Lett.* **96**, 221109 (2010).

<sup>19</sup>A. Divochyi, F. Marsili, D. Bitauld, A. Gaggero, R. Leoni, F. Mattioli, A. Korneev, V. Seleznev, N. Kurova, O. Minaeva, G. Gol'tsman, K. G. Lagoudakis, M. Benkhaoul, F. Lévy, and A. Fiore, *Nat. Photonics* **2**, 377 (2008).